Quantum dissipation in unbounded systems

Jeremy B. Maddox* and Eric R. Bittner†
Department of Chemistry, University of Houston, Houston, Texas 77204
(Received 31 August 2001; published 25 January 2002)

In recent years trajectory based methodologies have become increasingly popular for evaluating the time evolution of quantum systems. A revival of the de Broglie–Bohm interpretation of quantum mechanics has spawned several such techniques for examining quantum dynamics from a hydrodynamic perspective. Using techniques similar to those found in computational fluid dynamics one can construct the wave function of a quantum system at any time from the trajectories of a discrete ensemble of hydrodynamic fluid elements (Bohm particles) which evolve according to nonclassical equations of motion. Until very recently these schemes have been limited to conservative systems. In this paper, we present our methodology for including the effects of a thermal environment into the hydrodynamic formulation of quantum dynamics. We derive hydrodynamic equations of motion from the Caldeira-Leggett master equation for the reduced density matrix and give a brief overview of our computational scheme that incorporates an adaptive Lagrangian mesh. Our applications focus upon the dissipative dynamics of open unbounded quantum systems. Using both the Wigner phase space representation and the linear entropy, we probe the breakdown of the Markov approximation of the bath dynamics at low temperatures. We suggest a criteria for rationalizing the validity of the Markov approximation in open unbound systems and discuss decoherence, energy relaxation, and quantum/classical correspondence in the context of the Bohmian paths.

DOI: 10.1103/PhysRevE.65.026143 PACS number(s): 05.30.−d, 03.65.Yz

I. INTRODUCTION

The de Broglie–Bohm–Madelung description of quantum mechanics is based upon the observation that the quantum wave function ψ serves as an ancillary driving field for an ensemble of particle elements [1–6]. These so-called Bohmian trajectories are typically highly nonclassical since they follow the ray lines for a geometric construction of ψ [7]. In the causal interpretation of quantum mechanics, one can use a hydrodynamic analogy to ascribe some measure of physical reality to the individual trajectories. A detailed account of this view can be found in Refs. [8,9].

The hydrodynamic analogy of quantum mechanics is most naturally written in terms of the current density for a Madelung fluid defined by the probability distribution function given by $\rho(x)=|\psi(x)|^2$. In the Bohmian scheme, we represent the fluid by an ensemble of particles that follow a set of paths $x(t)$ satisfying $\dot{x}(t)=v[x(t)]$ which are identified as the flow lines (stream lines) of the probability fluid. As such, the velocity field for a particle of mass m is given by

$$\vec{v}(x,t)=\frac{\vec{j}(x,t)}{\rho(x,t)}, \tag{1}$$

where

$$\vec{j}(x,t)=\frac{\hbar}{2mi}(\psi^*\vec{\nabla}\psi-\psi\vec{\nabla}\psi^*) \tag{2}$$

is the current and $\rho(x)$ is the quantum density, which evolves according to the continuity equation:

$$\partial_t\rho+\vec{\nabla}\cdot\vec{j}=0. \tag{3}$$

Equations (1)–(3) are generally true for any fluid; however, for the case of a Madelung fluid we take ψ to be a solution of the time-dependent Schrödinger equation. Defining $d_t=\partial_t+v_\mu\partial_\mu$ as the material derivative that computes the rate of change along some path $\dot{x}_\mu(t)=v_\mu[x(t)]$, Eq. (3) becomes

$$\frac{1}{\rho}\frac{d\rho}{dt}=-(\partial_\mu v_\mu). \tag{4}$$

Consequently, given a discrete ensemble of space-time paths $\{x(t)\}$ we can define the wave function *pointwise* at any time t as

$$\psi(x(t))=\exp\left[-\int_0^t\partial_\mu v_\mu(s)ds\right]\exp\left[\frac{i}{\hbar}\int_0^t L(s)ds\right]\psi(x(0)), \tag{5}$$

where $\int_0^t L(s)ds$ is the action associated with the path $x(t)$. Written as such, we can clearly see from Eq. (5) that nonlocality and other intrinsically quantum mechanical effects are faithfully represented in this description. Substituting Eq. (5) into the time-dependent Schrödinger equation reveals that nothing has been swept under the rug. The wave function in Eq. (5) is a solution to the Schrödinger equation, it is simply that the propagator now acts pointwise over the space of quantum paths.

In the Bohmian description of quantum mechanics, it is generally argued that at some point these paths should resemble their classical analogues. Indeed, the action S obeys a Hamilton-Jacobi equation that is almost identical to the clas-

*Email address: jmaddox@uh.edu
†Email address: bittner@uh.edu

 ©2002 The American Physical Society

sical Hamilton-Jacobi equation with the addition of a nonlocal potential of purely quantum mechanical origin:

$$\partial_t S + H_{\text{class}} - \frac{\hbar^2}{2m}\frac{1}{\sqrt{\rho(x)}}\nabla^2\sqrt{\rho(x)} = 0. \tag{6}$$

The quantum potential represented in the last term represents a strain energy due to the local curvature of the quantum density. It does not depend upon the actual intensity of $\rho(x)$, only its shape. Consequently, trajectories are accelerated either through or away from regions of intense curvature. For a Gaussian wave packet, the quantum potential forces trajectories away from the central peak, thereby causing the wave packet to spread over as much space as possible thereby minimizing the strain energy. However, since Eq. (5) must be single valued along all the paths, the paths themselves are not allowed to cross each other. This gives rise to regions of compression and inflation within the wave function that can be easily identified with constructive and destructive interference. Hence individual Bohmian paths are typically nonclassical and generally bear no likeness whatsoever to their classical counter parts.

The purpose of this paper is to use the Bohmian construction to develop a quantum trajectory based theory suitable for studying systems at finite temperature. We have recently reported a Bohmian-like approach suitable for quantum Brownian motion as described by the reduced density matrix of a tagged harmonic oscillator in which the effects of the environment have been reduced to an effective influence action [10]. Our analysis involves two types of trajectories representing the evolution of the diagonal and off-diagonal elements of the density matrix and we address the questions: what (if any) effect an external environment plays in the evolution of a Bohmian trajectory and how can we correctly incorporate the effects of an external environment into a Bohmian description. Since Bohmian trajectories provide a suitable springboard for interpretation, we can use the trajectory construction as way to understand quantum relaxation, decoherence, and quantum/classical correspondence for a system in contact with a thermal bath.

In the present study, we focus our attention on the dissipative dynamics of unbounded quantum systems. Our interest in unbound systems is two part. First, the potential energy surface of an unbound system resembles the open channels of a reaction coordinate corresponding to the reactant and product species of a chemical reaction. We believe that our trajectory based approach might offer some novel insight into the fundamental difficulties associated with a quantum transition state theory for chemical reaction dynamics. To that end we pursue an understanding of dissipative effects on the Bohmian trajectories for several model unbounded systems. Secondly, the high-temperature limit of a system in contact with a thermal environment requires that the thermal energy of the bath be much greater than the zero-point energy of the system. This point becomes vague for unbounded systems where there is not necessarily a zero-point motion, leading us to conjecture an alternative criteria for rationalizing the domain of validity for high-temperature approximations in unbounded systems. In what follows, we present a brief overview of our approach and its implementation toward quantum dissipation in unbounded systems using adaptive-Lagrangian meshes.

II. THEORETICAL OVERVIEW

The starting point for our approach is to consider the dynamics of a quantum mechanical particle with mass m and position x in contact with a multimode bath with coordinates $\{q_1,\ldots,q_n\}$. The Lagrangian for such a system is given by

$$\mathcal{L} = \frac{m}{2}\dot{x}^2 - V(x) + \sum_{i=1}^{n}\left(\frac{m_i}{2}\dot{q}_i^2 - \frac{m_i\omega_i^2}{2}q_i^2\right) - \gamma x\sum_{i=1}^{n} c_i q_i\,. \tag{7}$$

Writing the full wave function for the combined ensemble as

$$|\psi(t)\rangle = e^{-iHt/\hbar}|\psi_s\rangle\otimes|\psi_B\rangle, \tag{8}$$

it is straightforward to infer that the velocity field in the system subensemble is given by

$$\vec{v}_s(x,\{q\},t) = \frac{\hbar}{2mi}\frac{[\Psi^*(x,\{q\},t)\partial_x\Psi(x,\{q\},t) - \text{c.c.}]}{|\Psi(x,\{q\},t)|^2}, \tag{9}$$

and that the velocity field for a member of the bath subensemble is given by

$$\begin{aligned}\vec{v}_{q_j}(x,\{q\},t) &= \dot{q}_j(x,\{q\},t)\\ &= \frac{\hbar}{2mi}\frac{[\Psi^*(x,\{q\},l)\partial_{q_j}\Psi(x,\{q\},t) - \text{c.c.}]}{|\Psi(x,\{q\},t)|^2}.\end{aligned} \tag{10}$$

Because the interaction coupling the system and the bath does not commute with either of the Hamiltonians representing the uncoupled evolution of the separated ensembles, the system trajectories $\dot{x}(t) = \vec{v}_s(t)$ are entangled with the evolution of the bath variables $\{q\}$ and vice versa. For a problem involving $O(10^{23})$ degrees of freedom the dynamics of this entangled system+bath state is quite intractable. We are thus forced to seek out a reduced description for the system dynamics. A wide variety of theoretical models have been developed for reducing the dimensions of a complex system. These include projection operator techniques, the Lindblad [11,12] semigroup operator approach, Redfield theory, the Feynman-Vernon [13,14] influence functional approach, fluctuating force models, and many others (cf., Ref. [15] for an excellent review). In this paper, we will invoke the influence functional approach that has produced several master equations [16–18] for the reduced density matrix of a quantum system in contact with a thermal bath. In the following subsections, we present a brief description of the simplest of these equations, the Caldeira-Leggett master equation, and also its hydrodynamic reformulation.

A. Caldeira-Leggett master equation

The motion of a classical particle in contact with a media is typically described using the Fokker-Planck equation to generate the various distribution functions characterizing the motion of an ensemble of trial trajectories. In particular, the velocity distribution of a particle undergoing Brownian motion evolves according to

$$\frac{\partial p(v,t)}{\partial t} = \gamma \frac{\partial}{\partial v}(v p(v,t)) + D_v \frac{\partial^2}{\partial v^2} p(v,t), \tag{11}$$

where $D_v = \gamma / M\beta$ and γ is the friction coefficient. If we apply the correspondence principle to this purely classical equation of motion, substituting the quantum mechanical operators $\hat{x}$ for x and $\hat{p}$ for p, one obtains a corresponding quantum mechanical version [19,20]

$$i\hbar \partial_t \rho = [\hat{H}_s, \rho] + \hbar i \gamma \left([\hat{x}, \{\hat{p}, \rho\}] - \frac{1}{\lambda^2} [\hat{x}, [\hat{x}, \rho]] \right). \tag{12}$$

Here, $\hat{H}_s = \hat{T}_x + V(\hat{x})$ is the renormalized system Hamiltonian with potential $V(\hat{x})$, $\hat{x}$ and $\hat{p}$ are the quantum mechanical position and momentum operators acting on the system and $\{\hat{A}, \hat{B}\} = \hat{A}\hat{B} + \hat{B}\hat{A}$ is the anticommutator bracket. Finally, $\lambda = \hbar / \sqrt{2mkT}$ is the thermal de Broglie wavelength for the particle of interest. Even though this simple substitution seems rather trivial and almost too obvious, Eq. (12) was in fact first derived by Caldeira and Leggett (CL) starting from a path-integral description for a particle coupled to a bath of harmonic oscillators [16]. As noted by many others, the CL equation is, *by construction*, strictly valid in the high-temperature limit where the zero-point motions in the bath can be effectively ignored. This approximation along with the assumption of a cutoff frequency for the spectral density ultimately leads to a Markovian description for the correlation of forces in the bath. As such, the CL model is valid only for times much longer than the characteristic relaxation time of the bath.

Working through the indicated operations in Eq. (12) produces a linear equation similar to the time-dependent Schrödinger equation

$$i\hbar \frac{\partial \rho}{\partial t} = L_\rho \rho, \tag{13}$$

where the Liouville operator L_ρ is an effective ''Hamiltonian'' operator for a quantum mechanical problem consisting of two degrees of freedom: x moving forward in time, and y moving backwards in time. Writing Eq. (13) explicitly, we find

$$L_\rho = H(x) - H(y) - i\hbar \gamma (x-y) \left(\frac{\partial}{\partial x} - \frac{\partial}{\partial y} \right) - i\gamma \left(\frac{2mkT}{\hbar} \right) (x-y)^2. \tag{14}$$

The first two terms in Eq. (14), $H(x) - H(y)$, we combine together as the quantum Liouvillian operator for the uncoupled system. The next term is the dissipative coupling to the environment. Indeed, the dynamics are much similar to that of a charged particle in a ''magnetic'' field with a vector potential

$$\vec{A} = \gamma (x-y)(\mathbf{i} - \mathbf{j}). \tag{15}$$

However, since $\vec{\nabla} \times \vec{A} = 0$ everywhere there no ''physical'' magnetic field. Finally, the last term in Eq. (14) reduces the magnitude of the off-diagonal elements of $\rho(x,y)$ bringing it to a diagonal form as $\rho(x,y)$ evolves in time. This we associate with the process of decoherence.

B. Quantum trajectories

Since we are interested in solving Eq. (13) by representing ρ as a Madelung fluid, we shall write ρ in the form suggestive of Bohmian mechanics for the quantum wave function

$$\rho(x,y) = e^{g + iA/\hbar}. \tag{16}$$

At this point, we move to a relative coordinate frame $\xi = (x+y)/\sqrt{2}$ and $\eta = (y-x)/\sqrt{2}$, whereby the components of the density matrix components along the ξ direction represent population at $x = y = \xi/\sqrt{2}$ and components in the η direction represent coherences between two spatially separated position eigenstates. Substituting $\rho(\xi, \eta)$ into Eq. (13) and using L_ρ from above, one obtains equations of motion for a Madelung fluid with two constitutive equations. First, an equation of continuity given by

$$\frac{dg}{dt} = -\frac{1}{2} \vec{\nabla} \cdot \vec{v} + \gamma - \frac{2\gamma}{\lambda^2} \eta^2. \tag{17}$$

Secondly, the Lagrangian

$$L = -m\dot{\xi}\dot{\eta} + 2m\gamma\eta\dot{\xi} - Q - V, \tag{18}$$

the time integral of which is the action A along a single quantum trajectory $z(t) = \{\xi(t), \eta(t)\}$ and is given by

$$A[z(t)] = \int_0^t L(z(t'), z(t') dt'. \tag{19}$$

The last two potential terms in Eq. (18) are the quantum potential $Q = Q(x) - Q(y)$ and classical potential $V = \tilde{V}(x) - \tilde{V}(y)$, which both come from the uncoupled Hamiltonian at two different points. The quantum potential in the relative frame is given by

$$Q = \frac{\hbar^2}{m} [\partial_{\xi,\eta} g + (\partial_\xi g)(\partial_\eta g)]. \tag{20}$$

In a dynamical sense, the strain energy of the Madelung fluid increases when the local curvature of the density increases. As we have noted earlier, this term introduces nonlocal coupling between trajectory elements and also represents a dif-

ferential geometric constraint between the extrinsic curvature invariants of a surface generated by $Z=cg(\xi,\eta)$ and the action per unit volume of a Lagrangian flow line of the Madelung fluid [21].

Given the action $A(\xi,\eta)$ and logarithmic amplitude $g(\xi,\eta)$, we can synthesize the density matrix over an ensemble of flow-line trajectories:

$$\rho(\xi(t),\eta(t),t)=\exp\left\{\int_0^t\left[-\frac{1}{2}\vec{\nabla}\cdot\vec{v}+\gamma-\frac{2\gamma}{\lambda^2}\eta^2(s)\right]ds+\frac{i}{\hbar}\int_0^t L\,ds\right\}\rho(\xi(0),\eta(0),0). \tag{21}$$

As in the analogous equation defining the wave function along a trajectory line, Eq. (21) may only be used *pointwise* on a space of discrete paths parameterized by *t*. In other words, at time $t=0$, we discretize ρ over an ensemble of points $\{\xi(0),\eta(0)\}$ and follow the evolution of ρ as the points themselves evolve as Lagrangian fluid elements. Because these trajectories are akin to the Bohmian trajectories of the wave function, we refer to the bundle of such trajectories as *Bohm-Liouville* trajectories.

To obtain the dynamics of the trajectory elements, we use the canonical relation between action and momentum, here defined as

$$p_\xi=-\frac{\partial S}{\partial\eta}, \tag{22}$$

$$p_\eta=-\frac{\partial S}{\partial\xi}. \tag{23}$$

This odd relation between the canonical momenta and the action is due to the time-reversed dynamics in the *y* direction introduced via the $\psi^*(y)$ contribution to the density matrix. Furthermore, since we have a vector potential present in the system, the material velocities and the canonical momenta are no longer parallel to each other, instead, the particle velocities are deflected by the vector potential

$$v_\eta=\dot{\eta}=\frac{p_\eta}{m}+2\gamma\eta, \tag{24}$$

$$v_\xi=\dot{\xi}=\frac{p_\xi}{m}. \tag{25}$$

Notice that all trajectories off the diagonal ξ axis of the density matrix are deflected *away* from the diagonal axis and trajectories originating on the ξ axis are constrained to remain on the ξ axis. This is simply a dynamical manifestation of the requirement that normalization of the density matrix be preserved, i.e.,

$$\frac{\partial}{\partial t}\mathrm{Tr}\,\rho=\frac{\partial}{\partial t}\int_{-\infty}^{\infty}\rho(\xi,0)\,d\xi=0. \tag{26}$$

What strikes one as quite odd is that the presence of dissipation via the vector potential seems to create long-ranged coherences within the system by pulling amplitude away from the diagonal ξ axis. However, this also has the effect of drawing density matrix amplitude into regions where the coherences are damped at an increasingly faster rate. The equilibrium state is achieved when these two processes counterbalance the effects of the quantum potential, leading to a stationary $\rho(\xi,\eta)$. While ρ may be stationary, the off-diagonal trajectories are certainly not stationary due to the cooperation of forces associated with the vector potential and finite curvature of the quantum density. We shall have more to say about this in a later section but for now we digress to discuss our computational methodology.

III. COMPUTATIONAL METHODOLOGY

Our computational scheme is based upon the quantum trajectory method (QTM) developed by Wyatt and coworkers for solving the time-dependent Schrödinger equation [21–25]. Recently Wyatt and Na [26] have extended their quantum trajectory based approach to a tagged oscillator in contact with an *n*-mode harmonic bath, (where $n\leqslant 15$) with each mode treated as an ensemble of Bohmian particles. This multidimensional treatment uses the trajectories as a moving Lagrangian mesh of points and synthesizes the wave function over the space of paths. This is in contrast to the typical post analysis where the wave function is first computed by solving the time-dependent Schrödinger equation and then the paths are computed. Other numerical applications of hydrodynamic trajectories in quantum mechanics can be found in Refs. [27,28].

Adapting the QTM for applications involving the density matrix is a fairly straightforward procedure and our implementation is as follows. The density matrix of a one-dimensional (1D) quantum system is discretized over a 2D grid of points. Each grid point represents a Lagrangian fluid particle that carries a bit of density $\exp(g)$ and phase *A*. The ensemble of particles obeys a set of Newtonian-type equations of motion determined by the forces associated with $\mathcal{Q}$, $\mathcal{V}$, and in general, the interactions with a thermal environment. This property of our approach is analogous to the ''quantum dressed'' classical mechanics scheme used by Billing [29–32] in cooperation with a time-dependent DVR methodology for solving the time-dependent Schrödinger equation.

The Bohm-Liouville particles are organized into local neighborhoods over which the functions and derivatives contained in Eq. (21) can be represented using a finite polynomial basis $\{p(\xi,\eta)\}$ and we use simple forward Eulerian integration to evaluate the time integrals. For a given neighborhood of points, we can expand a function $f(\xi,\eta)$ about some central point, (ξ_o,η_o), such that the value of the function at any point (ξ_i,η_i) in the neighborhood is given by

$$f(\xi_i,\eta_i)=f(\xi_o,\eta_o)+\sum_j^{n_b} a_j p_j(\xi_i-\xi_o,\eta_i-\eta_o), \tag{27}$$

where the a_j's are the coefficients for the polynomial basis. Typically we use a simple quadratic basis, i.e., $\{1,\xi,\eta,\xi^2/2,\xi\eta,\eta^2/2\}$ with approximately 10–20 points per

neighborhood. The fact that we have more neighborhood points than basis polynomials leads to an overdetermined set of least squares equations. In matrix notation this system of equations becomes $F=a\cdot p$, where $F_i=f(\xi_i,\eta_i)-f(\xi_o,\eta_o)$. The vector of coefficients is then determined for each point by finding the shape matrix p^{-1} such that $a=p^{-1}\cdot F$. Additionally, we incorporate a Gaussian weighting function such that neighboring points further away from (ξ_i,η_i) contribute less to the determination of its coefficients. It has been found that the weighting procedure enhances the locality of the polynomial fit thereby increasing the accuracy of the calculation. We also find it computationally beneficial to impose the symmetry requirements dictated by the Hermitian property of the density matrix. Specifically $A(\xi,\eta)$, $\mathcal{Q}(\xi,\eta)$, and $v_\eta(\xi,\eta)$ are all antisymmetric with respect to reflection across the η axis while $g(\xi,\eta)$ and $v_\xi(\xi,\eta)$ are symmetric. For a grid containing $n_\xi\times n_\eta$ points, we can reduce the computational overhead by explicitly propagating only the upper (or lower) half points.

The main advantage of the hydrodynamic approach is that the grid points in our calculations adapt to follow the flow of the quantum density whereas traditional Fourier techniques for solving the Liouville-von Neumann equation [33,34] are constrained to fixed spatial grids. Adaptation eliminates the need to have grid points in regions where there is no significant accumulation of density; however, as the density packet evolves into a once vacant region, the grid faithfully follows. Other numerical methodologies for examining the dynamics of dissipative quantum systems use Monte Carlo path integral schemes [35–37] for performing the highly nontrivial task of resolving an exact or approximate quantum propagator for the reduced system.

Unfortunately, there are several caveats that one encounters while using an adaptive Lagrangian grid. When the curvature of the density becomes intense the subsequent quantum forces are quite strong that often result in crossed trajectories: a phenomena that is strictly forbidden in the de Broglie–Bohm approach. This is referred to as the nodal problem and has been addressed by Wyatt and Bittner in Refs. [24,25]. A problem that is unique to dissipative systems is associated with the vector potential whereby particles are continuously deflected outward from the η axis resulting in a substantial loss of numerical accuracy. To combat this effect we find it necessary to periodically remesh the particles back onto a uniform grid. In bound systems, we have found that mapping the particles to a grid with dimensions defined by eight times the rms width of the density to be very successful. This method does not work so well for unbounded systems as the rms widths grow rapidly causing the mesh of particles to become very sparse as the grid expands. In the calculations that follow, we have imposed cut-off restrictions such that the dimensions of the grid will not expand beyond an arbitrary predetermined length. Combining the cut-off restrictions with the remeshing procedure ensures that the density of grid points is large enough to accurately compute the derivatives in the equations of motion. Eventually though the density becomes nonzero at the end points of the grid causing reflections that introduce spurious effects into our results. Nonetheless, despite this problem we are able to sustain sufficient numerical accuracy.

IV. DISCUSSION AND RESULTS

A. The free particle

Consider a free particle with mass m represented by a symmetric Gaussian density packet having initial rms widths given by $\sigma_\xi=\sigma_\eta=\sigma_o$. In the absence of any dissipative influence the Gaussian widths will expand according to the relation [38],

$$\sigma(t)=\sqrt{\langle x^2\rangle-\langle x\rangle^2}=\sigma_o\left(1+\frac{\hbar^2t^2}{4m^2\sigma_o^4}\right)^{1/2}. \tag{28}$$

The linear entropy of the system is related to the density matrix by the following expression:

$$S=-\mathrm{Tr}(\rho\ln\rho)\approx 1-\int\int_{-\infty}^{+\infty}\rho(\xi,\eta)\rho(\xi,-\eta)d\xi d\eta, \tag{29}$$

which for a Gaussian density packet is related to the rms widths by

$$S=1-\frac{1}{2}\frac{\sigma_\eta}{\sigma_\xi}. \tag{30}$$

For the nondissipative case, $S=1/2$ for all time since $\sigma_\xi=\sigma_\eta$. However, for dissipative dynamics we expect that $\sigma_\xi>\sigma_\eta$ due to narrowing of the density in η and broadening in ξ as a consequence of decoherence and relaxation. So we would predict that the linear entropy must be greater than one half for a free particle in contact with a thermal environment. We have analyzed the time dependence of the rms widths and the linear entropy for a free particle with mass $m=2000$ amu in contact with a thermal bath at various temperatures. In Fig. 1, we have plotted the curves for the linear entropy. The solid line represents the entropy for uncoupled case and we see that it does not vary with time. At high temperatures ($T\geqslant 800$ K), we observe that the curves for the linear entropy do increase in time and reflect the fact that σ_η is a decreasing function of time. This behavior is related to the destruction of phase information in the system and is the hallmark of decoherence in our calculations. At low temperatures ($T\leqslant 500$ K) the entropy actually *decreases* with time and in some cases (0 and 100 K) becomes less than zero, potentially violating the second law of thermodynamics. This result is somewhat suspicious in that the curves for σ_η dominate over those corresponding to σ_ξ. The odd behavior seems to suggest that at low temperatures, phase information actually flows into the system, a result that contradicts both the physical nature of decoherence and the fact that there cannot be coherence between states with zero population [38]. Notice that the entropy curves at 300 and 500 K plateau and eventually recross the undamped curve. This behavior indicates a time scale over which the CL model is not valid and demonstrates how that time scale decreases with increasing kT.

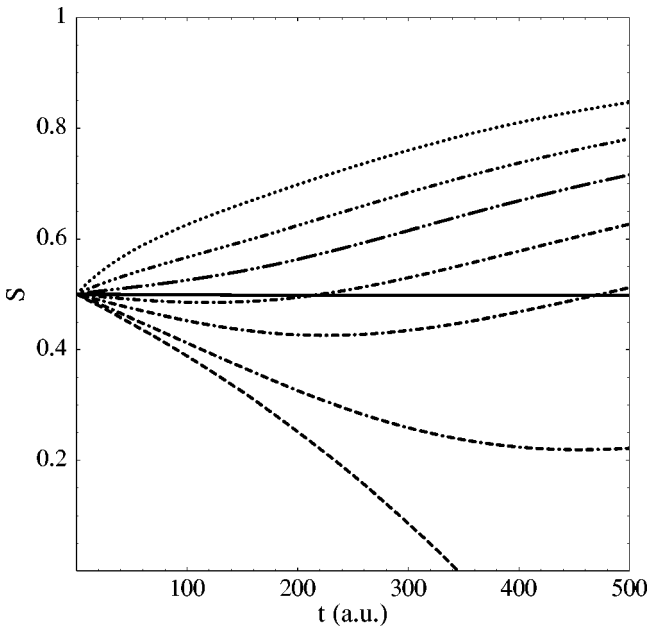

FIG. 1. Linear entropy vs time curves for the free particle, $m = 2000$ amu, in contact with a bath of harmonic oscillators with damping constant $\gamma = 0.005$ a.u.$^{-1}$ at temperatures (solid) $T = 0$ K, $(- - -)$ $T = 0$ K, $(\cdot - - -)$ $T = 100$ K, $(\cdot\text{--})$ $T = 300$ K, $(\cdot\cdot\text{--})$ $T = 500$ K, $(\cdots)$ $T = 800$ K, $(\cdots\text{-})$ $T = 1200$ K, and $(\cdot\ \cdot\ \cdot\ \cdot)$ $T = 2000$ K.

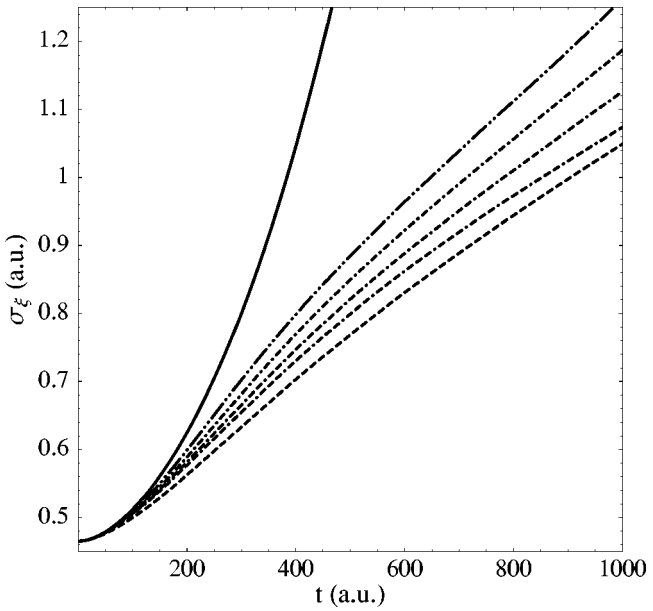

FIG. 2. σ_ξ vs time curves for a particle relaxing on the Eckart barrier at temperature (solid) $T = 0$ K, $(- - -)$ $T = 100$ K, $(\cdot - -)$ $T = 300$ K, $(\cdot\cdot\text{--})$ $T = 500$ K, $(\cdot\cdot\text{--})$ $T = 800$ K, and $(\cdots)$ $T = 1200$ K.

Another way that we can look at this is in terms of the Wigner representation of the density matrix. If we take the Wigner transform [39] of a Gaussian density matrix, we find that the width in η is inversely proportional to the spread in momentum of W_ρ. Setting $Q = \xi$, the Wigner transformation in the relative coordinate system is given by

$$W_\rho(Q,P) = \int \rho(Q,\eta) e^{iP\eta/\hbar} d\eta. \tag{31}$$

Taking

$$\rho(\xi,\eta) = A \exp\left[-\frac{1}{2}\left(\frac{\xi^2}{\sigma_\xi^2} + \frac{\eta^2}{\sigma_\eta^2} \right) \right], \tag{32}$$

as the form of a Gaussian density packet, where A is a normalization constant, the Wigner distribution is

$$W_\rho(Q,P) = \sqrt{2\pi}\sigma_\eta A \exp\left[-\frac{1}{2}\left(\frac{Q^2}{\sigma_\xi^2} + \frac{P^2\sigma_\eta^2}{\hbar^2} \right) \right]. \tag{33}$$

When $\langle Q \rangle = 0$ the uncertainty in position is given by the rms width $\Delta Q = \sigma_\xi$. For our Gaussian density packet, the uncertainty in momentum is then related to the uncertainty in η via a simple Fourier relationship, $\Delta P = \hbar/\sigma_\eta$. Looking at the undamped case we know that the uncertainty product, $\Delta Q \Delta P = \hbar \sigma_\xi / \sigma_\eta$ is preserved for all time. For the high-temperature cases, σ_ξ increases while σ_η decreases, hence the uncertainty product $\Delta Q \Delta P$ also increases. Furthermore, if the initial state were not a minimum uncertainty state (i.e., a squeezed state where $\sigma_\xi \neq \sigma_\eta$ at time $t = 0$) one could imagine the uncertainty product to decrease over the course of the decoherence time scale and then turnover to increase at some thermally prescribed rate. At low temperatures σ_ξ increases as before, however, σ_η increases at greater rate resulting in a "supercoherent" density matrix that violates Heisenberg's uncertainty principle, $\Delta Q \Delta P > \hbar$. Recall that the CL master equation is valid only in the limit of high temperature. Perhaps then it is not surprising that as we probe the lower bounds of this approximation, we subsequently violate several fundamental laws of physics. Our results serve as a demonstration of the well-known failure of the Markov approximation at low temperatures.

B. The symmetrical Eckart barrier

Next, we apply our methodology to the nontrivial problem of a wave packet relaxing on an Eckart barrier,

$$V(x) = V_o \,\mathrm{sech}^2(\pi x/\omega_o). \tag{34}$$

The Eckart barrier serves as a benchmark problem from transition state theory for modeling the reaction coordinate of a collinear $H + H_2$ reaction. Here we study the effects of dissipation on a Gaussian density packet centered about the peak of the barrier that is parameterized to resemble the $H + H_2$ reaction, where $V_o = 0.0249$ a.u. and $w_o = 0.6613$ a.u. We again examine the time dependence of the rms widths of the density packet and the linear entropy at various bath temperatures. The results for σ_ξ and σ_η are plotted in Figs. 2 and 3, respectively. The curves for the Eckart barrier exhibit the same general trends as the free particle problem. In the absence of a dissipative influence, the rms widths in ξ and η evolve identically for all time. For the high-temperature cases, we see evidence of decoherence as density amplitude

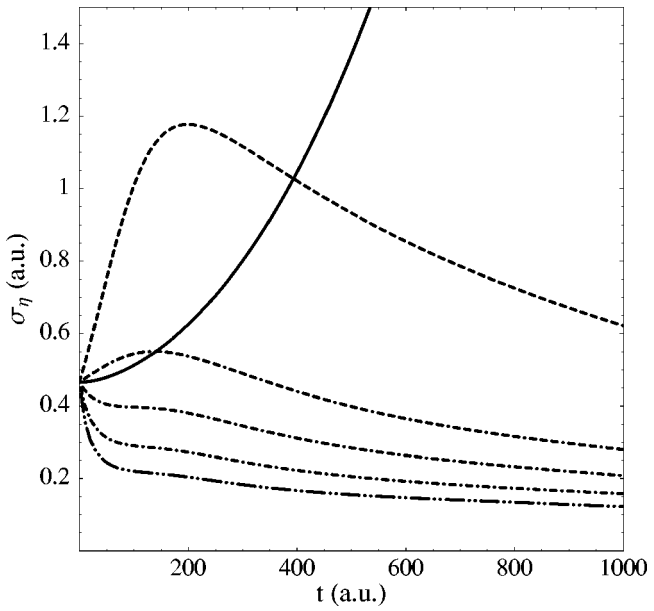

FIG. 3. σ_η vs time curves for the Eckart barrier at the temperatures using the same dashing scheme as in Fig. 2.

in η is damped down in time. At low temperatures, we observe that the curves for σ_η exceed that for the undamped scenario. As we have discussed, this nonphysical result suggests that the density matrix at finite temperature has become more coherent than the uncoupled system. After a certain point in time, we see that the low temperature σ_η curves eventually bottom out and recross the undamped solid line. Basically this corresponds to the emergence of a characteristic time scale over which the CL model is invalid. A similar type of analysis involving the linear entropy is given in Fig. 4. Because the density packet is not strictly a Gaussian for all

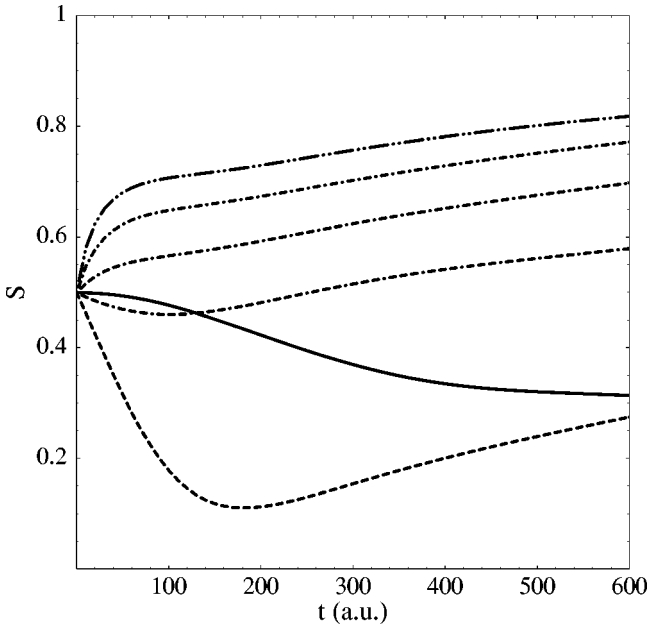

FIG. 4. Linear entropy vs time curves for the Eckart barrier at various temperatures using the same dashing scheme as in Fig. 2.

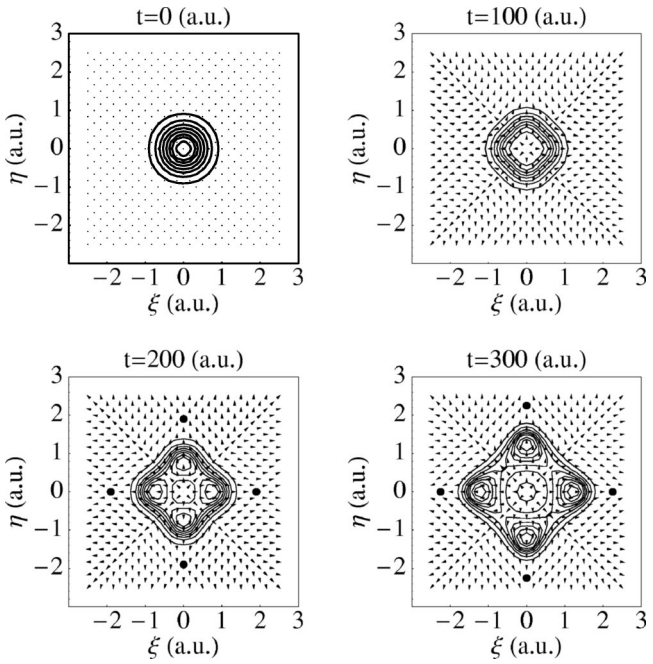

FIG. 5. Density contours and velocity field for an undamped particle, $m=2000$ amu. The density packet is initially a symmetric Gaussian having widths $\sigma_\xi=\sigma_\eta=0.2$ a.u., centered about the origin of an Eckart barrier parametrized for the $H+H_2$ reaction: $V_0=0.644$ a.u. and $w_0=0.661\,25$ a.u.

time, the linear entropy for the undamped case is no longer constant, however, the relative entropy reveals the same behavior as before. At high temperatures, the CL model is perfectly valid whereas at low temperatures we witness nonphysical behavior over a temperature dependent time scale for which there is a breakdown in the Markov approximation for the bath dynamics.

The second part of our analysis for the Eckart barrier involves the trajectories of the hydrodynamic particles. The contour plots in Figs. 5 and 6 illustrate how the quantum density $\exp(g)$ evolves in time and the corresponding vector field represents the material velocity field for the ensemble of the Lagrangian fluid particles. Figure 5 shows the uncoupled case where we see that the initial Gaussian gradually bifurcates into four distinct lobes. Notice that the density packet's evolution is fully coherent as the phase information in the system is preserved for all time. At zero time the particles are initially at rest; however, they are subject to the influence of both the classical and quantum forces so that the velocity field at nonzero time reflects the direction in which the particles are moving. Notice how as the packet splits, the velocity field tends to pull particles around to the leading edge of the forming lobes and that by time $t=200$ a.u. we can clearly see the formation of several focal points that are indicated by the filled circles. As the density packet evolves, the focal points advance outward pulling the density as they go. Allowing the particles to follow their natural paths would obviously result in a very distorted grid of points thus spoiling our attempts to estimate the various functions and derivatives contained in the equations of motion. We compensate for this by regularly mapping the particles back onto a rectangular

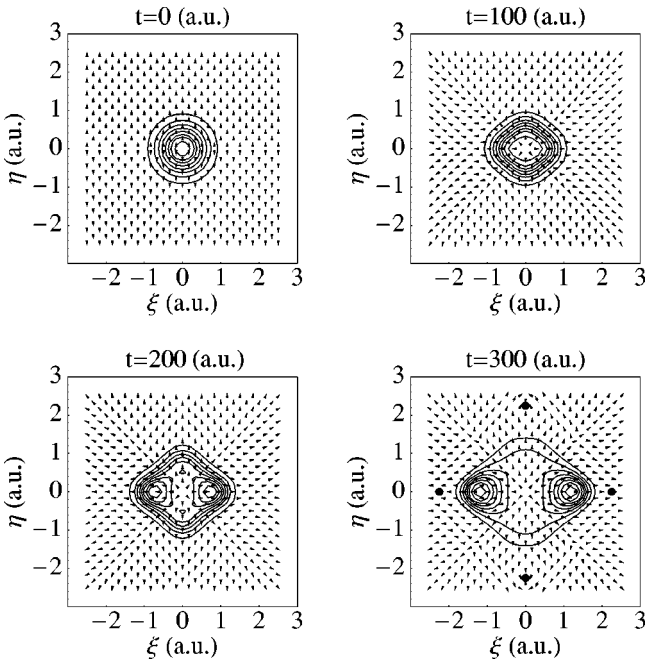

FIG. 6. Density contours and velocity field for the $H+H_2$ transition state with nonzero coupling, $\gamma=0.005$ a.u.$^{-1}$, to a thermal bath at temperature $T=1000$ K.

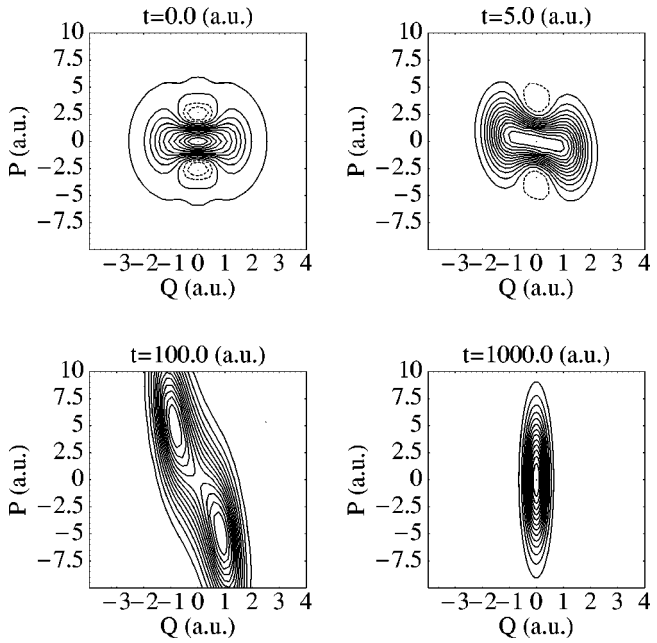

FIG. 7. Snapshots of the Wigner representation for a critically damped harmonic oscillator with mass $m=2000$ amu, period $\tau=888$ a.u., and temperature $T=1200$ K. Solid and dashed contours indicate positive and negative values, respectively. The initial state is a superposition of two coherent Gaussian wave packets separated by $d=1.5$ a.u.

grid of sufficient size to account for the expansion of the density packet. Figure 6 shows the case with nonzero coupling $\gamma=0.005$ a.u.$^{-1}$ to a bath of harmonic oscillators at finite temperature $T=1000$ K. The presence of the bath is immediately recognizable in the initial velocity field that is solely due to the influence of the dissipative vector potential. The evolution of the packet clearly shows the effects of decoherence as density amplitude in the η direction is depressed. At time $t=200$ a.u., we can see that there is a substantial amount of particle flow in the η direction corresponding to the expulsion of quantum phase information from the system. At longer times we would expect to observe the density packet to completely dissociate into several pieces that evolve more or less like a free particle with a nonzero group velocity.

C. Quantum/classical correspondence

It has been suggested that the Bohm interpretation fails to produce the correct classical limit only for systems isolated from the environment. This argument, first given by Bohm and Hiley [9] and later expanded upon by Appleby [40] states that if one can account for decoherence of the wave function, then the Bohmian paths should become more like their classical analogues. We find this notion to be incorrect and we feel that a clear distinction between Bohmian and classical trajectories is warranted. Since the idea of a coherence is absent in classical mechanics we shall be concerned with the Bohmian trajectories lying along the diagonal of the density matrix. These paths reflect the flow of probability in the system. The Wigner function is the appropriate representation for comparison with the probability distribution function of a corresponding classical system. Consider the case of a superposition state in a critically damped harmonic oscillator. The initial state is given by

$$\psi(x)=\frac{1}{\sqrt{2}}[\psi_g(x-x_o)+\psi_g(x+x_o)], \tag{35}$$

where $\psi_g(x)$ is a Gaussian wave packet. Figure 7 shows the evolution of the Wigner representation of this state. The solid and dashed curves represent positive and negative amplitude, respectively. After a few atomic time units the Wigner function does becomes completely positive and approaches the classical probability distribution function at longer times. However, we find that this does not imply that the trajectories of Bohmian particles bear any likeness whatsoever to classical trajectories. In fact, for this system the diagonal Bohmian trajectories become stationary, even at large displacements form the center of the harmonic well. This is in stark contrast to the behavior of classical trajectories that converge to the bottom of the well for the case of pure relaxation. This behavior is illustrated in Fig. 8. Figures 8(a) and 8(c) depict the Bohm trajectories in both phase space and coordinate space, respectively. Figures 8(b) and 8(d) are the corresponding classical trajectories for the same oscillator with pure dissipation. We see that the behavior of the Bohmian particles is obviously different from the classical trajectories. In the presence of thermal fluctuations, the classical particles obey a Langevin equation and we expect those trajectories to behave as random flights. From Fig. 8, it is clear that even though we have accounted for decoherence of the quantum system, the Bohmian trajectories do not bear any resemblance to classical trajectories.

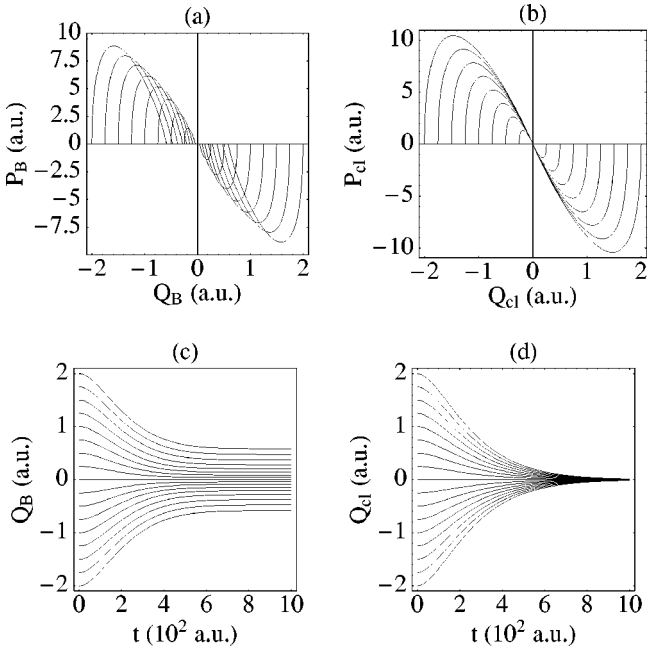

FIG. 8. Trajectories for a critically damped harmonic oscillator with mass $m=2000$ amu and period $\tau=888$ a.u. The trajectories are plotted for (a) diagonal Bohmian particles in phase space, (b) classical particles with pure dissipation in phase space, (c) diagonal Bohmian particles in position space (d) classical trajectories in position space.

V. CONCLUSIONS

The picture we are lead to is that the dissipative coupling to the environment causes a net flux of trajectory elements (representing population coherence information) toward $\eta \rightarrow \pm\infty$ and causes the populations along the ξ axis to relax to some lowest energy configuration. Furthermore, the coherence length as set by the de Broglie wavelength, becomes more and more short ranged as T increases causing the system to become localized in η, effectively diagonalizing the density matrix. In the equations-of-motion, both the quantum potential and the vector potential accelerate particles away from the diagonal axis. Consequently, even if the system were to become stationary (as in a bound system) as a result of some balance between the influx and efflux of energy, the off-diagonal trajectories themselves remain in constant motion reflecting the continuous entanglement between the system and bath degrees of freedom. This continual "production" of coherence is ultimately traced to the nonlocal nature of the quantum potential. In essence, pure decoherence tries to force $\rho(\xi, \eta)$ into a sharp Gaussian about the population axis. However, as $\rho(\xi, \eta)$ becomes sharply curved about $\eta=0$, the quantum potential begins to increase and forces ρ to broaden in η–thereby producing longer-ranged coherences. Consequently, an equilibrium is established when the squeezing due to decoherence is counterbalanced by the outward pressure of the quantum force. Furthermore, even at times on the order of the relaxation time scale we find that Bohmian trajectories behave differently from classical trajectories. This strengthens the assertion that Bohm paths and classical paths are fundamentally incongruous even postdecoherence.

At high temperatures, we find that our results for both the free particle and Eckart barrier fit very nicely into this picture of quantum dissipation. Contradictory evidence at low temperatures can be ascribed to the well-known breakdown of the Markov approximation on short time scales. The domain of validity for the Markov approximation is related to the temperature of the bath and the system-bath coupling. Typically the Markov approximation is assumed to be valid in the limit of high temperature that is usually applied by assuming that the thermal energy of the bath is very much greater than the zero-point energy of the system. In some sense this limit excludes unbounded systems where the distribution of energy states is continuous rather than discrete. We suggest a more general criteria that is necessary but not sufficient for determining the domain of validity for high-temperature approximations: at any instant in time, the reduced density matrix for a system at finite temperature must never be more coherent than the uncoupled system. This generalization simply states that the upper bound for the degree of localization in η (i.e., σ_η) for a system at finite temperature at a given time is dictated by the corresponding uncoupled system.

[1] D. Bohm, Phys. Rev. **85**, 166 (1952).
[2] D. Bohm, Phys. Rev. **85**, 180 (1952).
[3] L. de Broglie, C. R. Acad. Sci. Paris **183**, 24 (1926).
[4] L. de Broglie, Nature (London) **118**, 441 (1926).
[5] L. de Broglie, C. R. Acad. Sci. Paris **184**, 273 (1927).
[6] E. Madelung, Z. Phys. **40**, 322 (1926).
[7] V. I. Arnold, *Mathematical Methods of Classical Mechanics* (Springer, New York, 1989).
[8] P. R. Holland, *The Quantum Theory of Motion* (Cambridge University Press, Cambridge, England, 1993).
[9] D. Bohm and B. Hiley, *The Undivided Universe* (Routledge and Kegan Paul, London, 1993).
[10] J. B. Maddox and E. R. Bittner, J. Chem. Phys. **115**, 6309 (2001).
[11] R. Kosloff and S. A. Rice, J. Chem. Phys. **72**, 4591 (1980).
[12] G. Lindblad, Commun. Math. Phys. **48**, 119 (1976).
[13] R. P. Feynman and F. L. Vernon, Ann. Phys. (N.Y.) **24**, 118 (1963).
[14] R. P. Feynman and A. R. Hibbs, *Quantum Mechanics and Path Integrals* (McGraw-Hill, New York, 1965).
[15] D. Kohen, C. C. Marston, and D. J. Tannor, J. Chem. Phys. **107**, 5236 (1997).
[16] A. O. Calderia and A. J. Leggett, Physica A **121**, 587 (1983).
[17] W. G. Unruh and W. H. Zurek, Phys. Rev. D **40**, 1071 (1989).
[18] B. L. Hu, J. P. Paz, and Y. Zhang, Phys. Rev. D **45**, 2843 (1992).
[19] B. Vacchini, Phys. Rev. Lett. **84**, 1374 (2000).
[20] B. Vacchini, Phys. Rev. E **63**, 066115 (2001).
[21] E. R. Bittner, J. Chem. Phys. **112**, 9703 (2000).
[22] R. E. Wyatt, J. Chem. Phys. **111**, 4406 (1999).

[23] C. L. Lopreore and R. E. Wyatt, Phys. Rev. Lett. **82**, 5190 (1999).
[24] R. E. Wyatt and E. R. Bittner, J. Chem. Phys. **113**, 8888 (2000).
[25] E. R. Bittner and R. E. Wyatt, J. Chem. Phys. **113**, 8898 (2000).
[26] Y. Na and R. E. Wyatt, Phys. Rev. E **65**, 016702 (2002).
[27] B. K. Dey, A. Askar, and H. Rabitz, J. Phys. Chem. **109**, 8770 (1998).
[28] J. C. Burant and J. C. Tully, J. Chem. Phys. **112**, 6097 (2000).
[29] G. D. Billing, Chem. Phys. Lett. **339**, 237 (2001).
[30] G. D. Billing, Chem. Phys. **264**, 71 (2001).
[31] G. D. Billing, J. Chem. Phys. **114**, 6641 (2001).
[32] G. D. Billing, J. Phys. Chem. A **105**, 2340 (2001).
[33] M. Berman and R. Kossloff, Comput. Phys. Commun. **63**, 1 (1991).
[34] M. Berman, R. Kossloff, and H. Tal-Ezer, J. Phys. A **25**, 1283 (1992).
[35] M. Topaler and N. Makri, J. Chem. Phys. **101**, 7500 (1994).
[36] N. Makri, J. Math. Phys. **36**, 2430 (1995).
[37] J. Cao, L. W. Ungar, and G. A. Voth, J. Chem. Phys. **104**, 4189 (1999).
[38] C. Cohen-Tannoudji, B. Diu, and F. Laloe, *Quantum Mechanics* (Wiley Interscience, New York, 1977).
[39] E. P. Wigner, Phys. Rev. **40**, 749 (1932).
[40] D. M. Appleby, e-print quant-ph/9908029.